Journal of Sustainable Metallurgy (2018) 4:443–454
https://doi.org/10.1007/s40831-018-0190-4

RESEARCH ARTICLE

Effect of Fe^{2+}/T.Fe Ratio on the Dissolution Behavior of P from Steelmaking Slag with High P_2O_5 Content

Chuan-ming Du[1] · Xu Gao[1] · Shigeru Ueda[1] · Shin-ya Kitamura[1]

Published online: 19 September 2018

Abstract
Steelmaking slag with high P_2O_5 content is generated when using high-P iron ores. This slag primarily consists of a CaO–SiO_2–FeO–Fe_2O_3–P_2O_5 system and is regarded as a potential P source. To separate and recover P, selective leaching of the P-concentrated solid solution from steelmaking slag was employed. To determine the appropriate slag composition for selective leaching, it is necessary to clarify the influence of the molar ratio of Fe^{2+} to total Fe (Fe^{2+}/T.Fe) on the dissolution behavior of steelmaking slag. This study found that as the Fe^{2+}/T.Fe ratio in slag increased, the P_2O_5 content in the solid solution decreased, while the mass fraction of the solid solution increased; therefore, most of the P was still distributed in the solid solution. During leaching, citric acid showed an enhanced capacity to dissolve P from slag. When nitric acid is used as leaching agent, leaching should be conducted at a lower pH to achieve a leaching performance similar to that of citric acid. Because the presence of FeO in the solid solution deteriorated its dissolution, the dissolution ratio of P decreased significantly with the increasing Fe^{2+}/T.Fe ratio in slag. By contrast, the dissolution of Fe was promoted. This was attributed to a higher dissolution of the CaO–SiO_2–FeO matrix phase compared with the CaO–SiO_2–Fe_2O_3 matrix phase. Therefore, to achieve a better selective leaching of P, steelmaking slag should be oxidized to lower the Fe^{2+}/T.Fe ratio below 0.1.

Keywords High-P iron ores · Steelmaking slag · Fe^{2+}/T.Fe · Selective leaching · C_2S–C_3P solid solution

Introduction

The development of the iron and steel industry has been restricted due to the gradual decrease in reserves and the consistently increasing price of high-grade (< 0.075 mass% P) iron ores [1]. To solve this crisis, many attempts have been devoted to the utilization of low-grade iron ores, such as high-P iron ores in massive reserves [2, 3]. Because P is detrimental to the low-temperature toughness of steel products, most of the P present in iron ores or hot metal should be removed during the ironmaking or steelmaking process. In general, high-P iron ores are dephosphorized by acid leaching or pre-reduction prior to their use in smelting [3, 4]. Although the P content of high-P iron ores is far lower than that in phosphate ores, the total amount of P in high-P iron ores is considerably large due to its huge consumption. From another perspective, if P can be enriched and then effectively separated, these P will be an alternative source to secure P supplies. Value-added utilization of high-P iron ores and sustainable steelmaking are achievable.

During dephosphorization, the P in hot metal that originates in the iron ores is oxidized and then transferred to the slag. This is also regarded as a P enrichment process. P is mainly distributed in the $2CaO{\cdot}SiO_2$–$3CaO{\cdot}P_2O_5$ (C_2S–C_3P) solid solution [5, 6]. When high-P iron ores are utilized, hot metal with high P content will be generated. Iron ores containing 0.1 mass% or more P have already been used in India, and the P content in hot metal exceeded 0.25 mass% [7, 8]. To meet the demands for low-P steel, a highly efficient dephosphorization process is necessary. Kitamura et al. [9] studied the dephosphorization treatment of hot metal with high P content. It was determined that the P content in steel could decrease from 0.3 to 0.015 mass %

The contributing editor for this article was Veena Sahajwalla.

✉ Chuan-ming Du
dcm198812@gmail.com

[1] Institute of Multidisciplinary Research for Advanced Materials, Tohoku University, 2-1-1 Katahira, Aoba-ku, Sendai, Miyagi 980-8577, Japan

in hot metal, and slag containing more than 10 mass% P_2O_5 could generate based on a simulation model. Furthermore, the addition of Na_2O to slag can increase the phosphate capacity of slag and enhance the distribution ratio of P [10, 11]. These results demonstrated that dephosphoriztion of hot metal with high P content and formation of slag with high P_2O_5 content are achieved.

The P concentrated in slag with high P_2O_5 content is regarded as a potential P source. Separation and recovery of P from steelmaking slag has been studied by many researchers [12, 13]. Based on the difference in solubility between the C_2S–C_3P solid solution and CaO–SiO_2–Fe_tO matrix phase in the aqueous solution, Teratoko and Kitamura et al. [14] proposed the selective leaching of P from steelmaking slag. The dissolution ratios of each element from the matrix phase were lower than those from the solid solution, and the solid solution in steelmaking slag was selectively dissolved at a constant pH [15]. It was expected that the dissolved P in the leachate would be a suitable raw material for the production of phosphate fertilizer since this process was similar to the wet process for producing phosphate fertilizers [16]. Furthermore, the remaining P-poor and Fe-rich mineralogical phase could be recycled for further use in a steelmaking plant. Previously, we have studied the dissolution behavior of P from steelmaking slag with high P_2O_5 content, which consisted of a CaO–SiO_2–Fe_2O_3–P_2O_5 system [17–20]. It was determined that slow cooling of the molten slag and Na_2O modification was necessary to realize the selective leaching of P from slag because they not only promoted the dissolution of the P-concentrated solid solution but also suppressed the dissolution of the Fe-rich matrix phase. Therefore, most of the P in slag was dissolved without Fe significantly dissolving.

However, the practical steelmaking slag primarily consists of the CaO–SiO_2–FeO–Fe_2O_3–P_2O_5 system. The valence of Fe in slag has a significant influence on the dissolution of slag. It has been reported that when FeO was used as the iron oxide, the dissolution ratio of P from slag was much lower than when Fe_2O_3 was used [14]. In addition, the matrix phase of the CaO–SiO_2–FeO system was more easily dissolved compared to that of the CaO–SiO_2–Fe_2O_3 system [21]. To determine the appropriate slag composition for selective leaching, it was necessary to clarify the effect of the molar ratio of Fe^{2+} to total Fe (Fe^{2+}/T.Fe) in slag on the dissolution behaviors of P and Fe. In this study, five types of slags with different Fe^{2+}/T.Fe ratios were synthesized, and their dissolution behaviors in the citric and nitric acid solutions were investigated, respectively.

Experimental Method

Reagent-grade CaO, SiO_2, Fe_2O_3, $Ca_3(PO_4)_2$, FeO, and Na_2SiO_3 were used to synthesize the slag containing the CaO–SiO_2–FeO–Fe_2O_3–P_2O_5 system. CaO was produced by calcining $CaCO_3$ in an Al_2O_3 crucible at 1273 K for 10 h. To synthesize FeO, electrolytic Fe powder and Fe_2O_3 were fully mixed in a 1:1 molar ratio, and then heated to 1723 K in a Fe crucible under Ar atmosphere. Table 1 lists the compositions of slags with different Fe^{2+}/T.Fe ratios. These slags have the same total Fe content and basicity ((mass% CaO)/(mass% SiO_2)). To promote the dissolution of P, Na_2O was added as a modifier [18]. The P_2O_5 and Na_2O contents in each slag were fixed at 8 and 4 mass %, respectively. According to the target compositions, 10 g of the oxides were thoroughly mixed and heated to form a homogeneous liquid phase. To fabricate slag A, containing only Fe_2O_3, the sample was heated to 1773 K in a Pt crucible in air. To produce slag E, which contained only FeO, the sample was heated to 1723 K (below the melting point of crucible) in an Fe crucible in Ar. To manufacture the slags containing Fe_2O_3 and FeO (slags B, C, and D), the samples were heated to 1773 K in Pt crucibles under a CO_2–CO gas mixture, which was used to control the partial pressure of oxygen. To estimate the CO_2/CO volume ratio in each case, the activities of FeO and Fe_2O_3 in the molten slag were first calculated using the Factsage 7.0 software. Subsequently, the partial pressure of oxygen was calculated using Eq. (1) [22]. The CO_2/CO volume ratios were determined using Eq. (2) [23] and presented in Table 1. As shown in Fig. 1, the liquid slags were cooled to 1623 K and kept at this temperature for 20 min to precipitate the solid solution. After heating, the samples were cooled in the furnace at a cooling rate of 5 K/min and removed from the furnace after reaching 1323 K.

Table 1 Initial compositions of slags with different Fe^{2+}/T.Fe ratios (mass%) obtained using different synthesis conditions

Sample	CaO	SiO_2	Fe_2O_3	FeO	P_2O_5	Na_2O	Fe^{2+}/T.Fe	Crucible	Atmosphere
Slag A	33.5	22.3	32.2	0	8.0	4.0	0	Pt	Air
Slag B	34.0	22.6	24.1	7.3	8.0	4.0	0.25	Pt	CO_2:CO = 50:1
Slag C	34.5	22.9	16.1	14.5	8.0	4.0	0.50	Pt	CO_2:CO = 5:1
Slag D	35.0	23.2	8.1	21.7	8.0	4.0	0.75	Pt	CO_2:CO = 1:1
Slag E	35.4	23.6	0	29.0	8.0	4.0	1.00	Fe	Ar

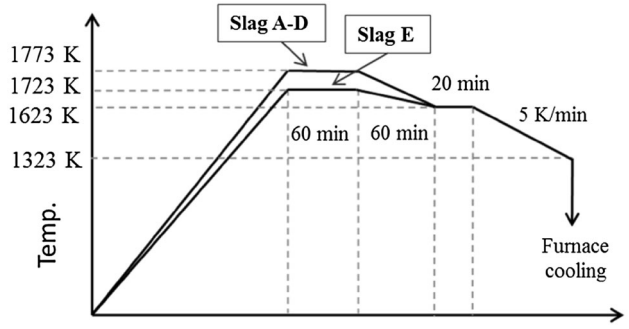

Fig. 1 Experimental conditions for slag synthesis

The elemental compositions of the slags were determined using inductively coupled plasma atomic emission spectroscopy (ICP-AES). The Fe^{2+} content in the slags was determined by potassium dichromate titration [24]. The mineralogical compositions of the slags were analyzed using electron probe microanalysis (EPMA) and X-ray diffraction (XRD) analysis.

$$2\mathrm{FeO(l)} + \frac{1}{2}\mathrm{O_2(g)} = \mathrm{Fe_2O_3(s)}\ \Delta G^{\circ} = -334585 + 153.32T\mathrm{J/mol} \quad (1)$$

$$\mathrm{CO(g)} + \frac{1}{2}\mathrm{O_2(g)} = \mathrm{CO_2(g)}\ \Delta G^{\circ} = -281000 + 85.23T\mathrm{J/mol} \quad (2)$$

The synthesized slags were ground into particles smaller than 53 μm and used for the leaching experiments. The leaching apparatus was the same as that used in previous studies [17]. We added 1 g slag to 400 mL distilled water and agitated the mixture using a rotating stirrer at 200 rpm. The temperature of the aqueous solution was kept at 298 K using an isothermal water bath. During slag dissolution, Ca^{2+} ions dissolved into the aqueous solution, which caused an increase in pH. Acid solution was automatically added to keep the pH constant. In this study, citric acid ($H_3C_6H_5O_7$, 0.1 mol/L) was used as leaching agent, and compared with nitric acid (HNO_3, 0.2 mol/L). To achieve more efficient selective leaching of P, the pH was determined based on previous studies [18, 20]. Each slag was leached using citric acid at pH 6 and nitric acid at pH 4, respectively. The leaching time was set as 120 min. Approximately 5 mL of aqueous solution was sampled at adequate intervals and filtered using a syringe filter (< 0.45 μm). The concentration of each element in the filtered solution was determined using ICP-AES. After leaching, the undissolved slag was collected by filtering the aqueous solution. The dried residue was weighed and analyzed using XRD and EPMA.

Table 2 Analyzed Fe^{2+}/T.Fe molar ratio of each slag

Sample	Slag A	Slag B	Slag C	Slag D	Slag E
Fe^{2+}/T.Fe molar ratio	0	0.368	0.590	0.729	1.000

Results and Discussion

Table 2 lists the analyzed Fe^{2+}/T.Fe molar ratios of all slags obtained after sample preparation. Compared with the designed ratios, the actual Fe^{2+}/T.Fe ratios of slags B and C were higher, resulting from lower partial pressure of oxygen (lower CO_2/CO volume ratio) during slag synthesis. The actual Fe^{2+}/T.Fe ratio of slag D was close to the designed value.

Mineralogical Composition

Typical cross sections of slags with different Fe^{2+}/T.Fe ratios are shown in Fig. 2. Table 3 lists the average composition of each phase in these slags. Each slag mainly consisted of three phases. The white phase, rich in Fe_tO, was wüstite or hematite (Fe-rich phase). The black phase, which contained a higher P_2O_5 content, was the solid solution. The gray phase of the CaO–SiO_2–Fe_tO system was considered the matrix phase. It can be seen that for slag E, which contained FeO, the particles of the solid solution were larger than those for slag A, which contained Fe_2O_3, while the particles of the Fe-rich phase were smaller. The composition of the Fe-rich phase was almost the same in these slags. With the increasing Fe^{2+}/T.Fe ratio in slag, the P_2O_5 and Na_2O contents in the solid solution decreased, but Fe_tO became easier to be distributed in the solid solution. The P_2O_5 content in the solid solution of slag E decreased to 19.3 mass%, while the FeO content in it reached 7.0 mass%. The P_2O_5 and Na_2O contents in the matrix phase were not significantly different for these slags. Higher Fe^{2+}/T.Fe ratios in slags led to lower CaO and higher Fe_tO contents in the matrix phase. Figure 3 shows the change in the distribution ratios of P_2O_5 and Na_2O between the solid solution and matrix phase. Most of the P_2O_5 was concentrated in the solid solution because of the higher distribution ratio of P_2O_5 in each slag. The distribution ratio of P_2O_5 increased with the decrease in the Fe^{2+}/T.Fe ratio in slag. The slags with lower Fe^{2+}/T.Fe ratios showed higher distribution ratio of Na_2O, yet their values were smaller than 2.

Dissolution Behavior of Slag

Figure 4 shows the changes in the concentrations of Ca, P, and Fe in the citric acid solution at pH 6. The concentration of each element increased continuously with the leaching

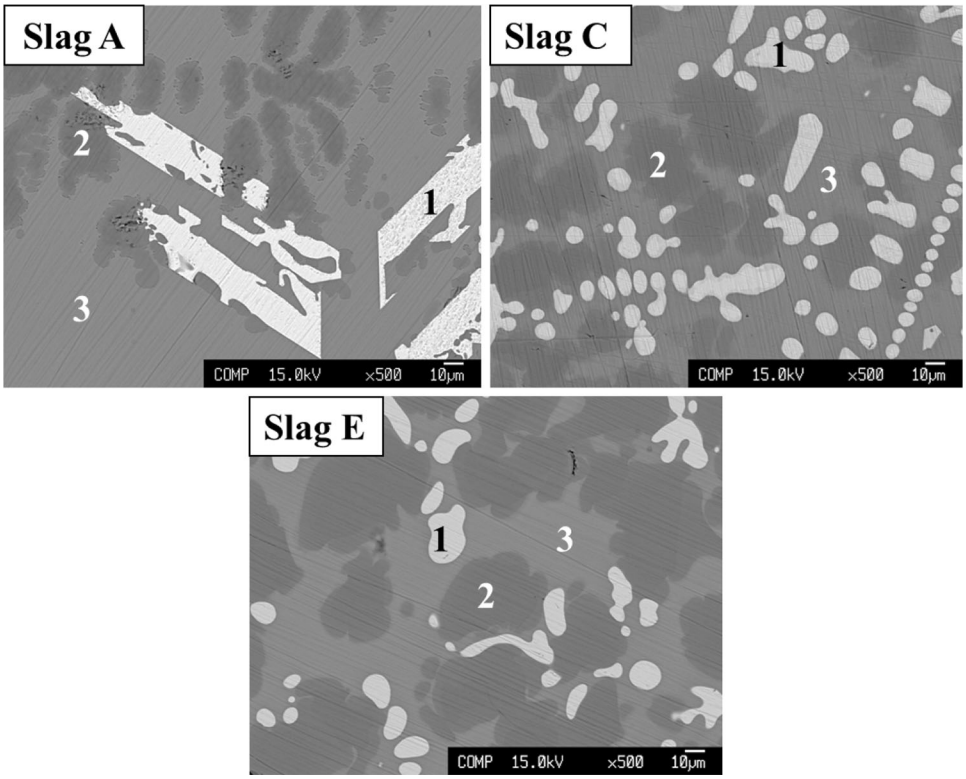

Fig. 2 Typical cross sections of slags with different Fe^{2+}/T.Fe ratios

Table 3 Average compositions of each phase in slags with different Fe^{2+}/T.Fe ratios (mass%)

	CaO	SiO_2	Fe_tO	P_2O_5	Na_2O
Fe-rich phase (wüstite and hematite)					
Slag A	0.2	0.0	99.8	0.0	0.0
Slag B	0.7	0.1	99.2	0.0	0.0
Slag C	0.5	0.1	99.3	0.0	0.0
Slag D	0.6	0.1	99.2	0.1	0.0
Slag E	0.5	0.1	99.4	0.0	0.1
C_2S–C_3P solid solution					
Slag A	48.0	10.1	0.7	33.4	7.7
Slag B	48.7	15.1	2.8	26.1	7.3
Slag C	49.4	19.4	5.3	20.1	5.9
Slag D	49.2	20.1	5.8	19.2	5.7
Slag E	47.4	20.7	7.0	19.3	5.6
CaO–SiO_2–Fe_tO matrix phase					
Slag A	36.2	36.8	21.2	1.5	4.3
Slag B	34.2	39.0	21.0	1.3	4.5
Slag C	30.4	37.2	26.9	1.0	4.5
Slag D	29.2	36.1	29.0	1.3	4.4
Slag E	27.9	36.0	30.7	1.6	3.9

time. However, the dissolution rate of slag obviously decreased after 60 min, causing small increases in the concentrations. Ca concentration was the highest of all the dissolved elements. After 120 min, Ca concentration was almost the same for all slags, reaching approximately 280 mg/L. For slag A, which contained Fe_2O_3, Fe concentration was very low, on the order of only several mg/L; however, it increased significantly as the Fe^{2+}/T.Fe ratio in slag increased. When the Fe^{2+}/T.Fe ratio exceeded 0.59, Fe concentration was higher than 100 mg/L. A further increase in the Fe^{2+}/T.Fe ratio did not lead to a significant increase in Fe concentration. Compared with Fe, P

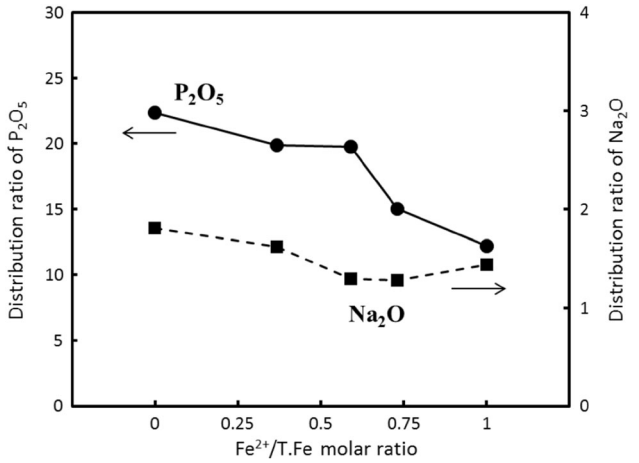

Fig. 3 Distribution ratios of P_2O_5 and Na_2O between the solid solution and matrix phase for slags with different Fe^{2+}/T.Fe ratios

exhibited an opposite dissolution behavior. The dissolution of P from slag A was the fastest in the initial period, when we determined the highest P concentration. Increasing the Fe^{2+}/T.Fe ratio in slag decreased P concentration. For slags with higher Fe^{2+}/T.Fe ratios, P concentration was less than 20 mg/L after 120 min.

On the basis of the compositions of the final leachates, the dissolution ratio of each element from different slags was calculated using Eq. (3):

$$R_{\mathrm{M}} = \frac{C_{\mathrm{M}} \cdot V}{m_{\mathrm{M}}}, \tag{3}$$

where R_{M} is the dissolution ratio of element M from slag, C_{M} is the concentration of M after 120 min (mg/L), V is the final volume of the aqueous solution (L), and m_{M} is the mass of M in 1 g of slag (mg). Figure 5 shows the calculated results in the citric acid solution at pH 6. The dissolution ratios of Ca and Na from each slag were almost the same, reaching approximately 45% and 55%, respectively. Approximately 80% of P was dissolved from slag A, which contained only Fe_2O_3, while the dissolution of Fe was negligible. Increasing the Fe^{2+}/T.Fe ratio in slag significantly suppressed the dissolution of P and promoted the dissolution of Fe, which deteriorated the selective leaching of P. When the Fe^{2+}/T.Fe ratio in slag was higher than 0.59, the difference in dissolution ratios of P, Fe, and Si was insignificant. For slag E, which contained only FeO, only 17.0% of P was dissolved, while the dissolution ratio of Fe increased to 21.4%. In addition, the dissolution ratio of Si almost doubled compared with slag A.

The dissolution behavior of Ca, Fe, and P when nitric acid was used as leaching agent at pH 4 is shown in Fig. 6. The changes in the concentrations of each element with leaching time were similar to those in the citric acid solution at pH 6. Slag A, which contained only Fe_2O_3, showed the lowest Ca concentration. For the slags

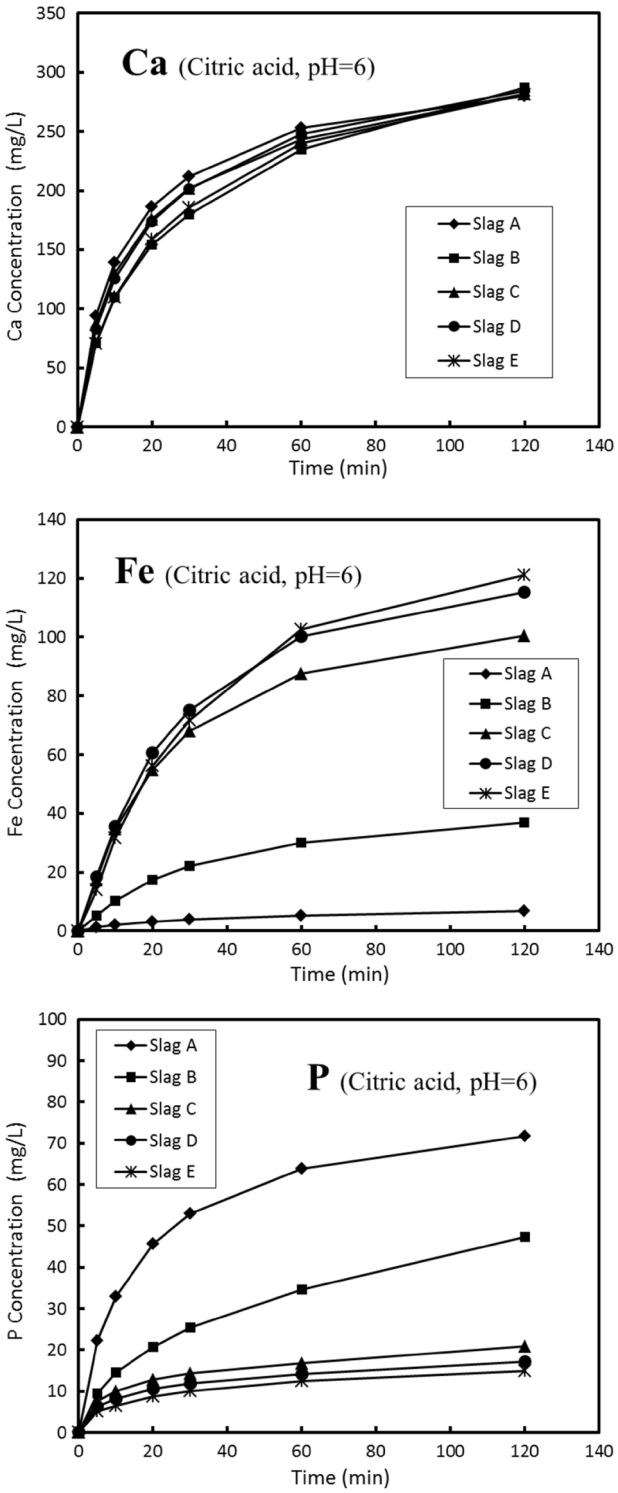

Fig. 4 Changes in Ca, Fe, and P concentrations in the citric acid solution at pH 6

containing FeO, Ca concentrations were very close, exceeding 450.0 mg/L. Fe concentration increased with the increasing Fe^{2+}/T.Fe ratio in slag, and reached 112.8 mg/L when only FeO existed in slag. For the slags where the Fe^{2+}/T.Fe ratio was larger than 0.59, the concentration of P

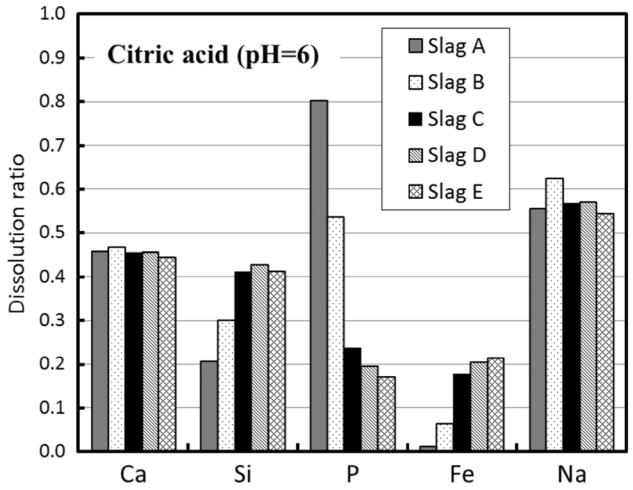

Fig. 5 Dissolution ratios of each element from different slags at pH 6 (citric acid solution)

was almost the same, and less than 20.0 mg/L. As the Fe^{2+}/T.Fe ratio decreased, the dissolution of P increased significantly and could reach 68.6 mg/L after 120 min.

Using the above concentrations and Eq. (3), the dissolution ratios of each element from different slags in the nitric acid solution were calculated. Figure 7 shows that when only Fe_2O_3 existed in slag, the dissolution ratio of P was the highest, and the dissolution ratios of other elements were lower. Thus, it exhibited a better selective leaching of P, similar with that in the citric acid solution at pH 6. When the Fe^{2+}/T.Fe ratio in slag increased to 0.59, there was a sharp decrease in the dissolution ratio of P. By contrast, the dissolution of other elements was significantly promoted. The majority of Ca, Si, and Na were dissolved, and the dissolution ratio of Fe increased to 16.4%. A further increase in the Fe^{2+}/T.Fe ratio had an insignificant influence on the dissolution of slag. For slag E, the dissolution ratio of P was only 21.0%, which was far lower than those of Ca and Si.

Citric acid can dissolve minerals via two possible mechanisms [25]: the direct displacement of metal ions from the mineral matrix by hydrogen ions and formation of soluble metal complexes and chelates. These mechanisms result in a higher dissolution ratio of P from steelmaking slag in nearly neutral aqueous solutions. When nitric acid was used as leaching agent, to achieve a leaching performance similar to that in citric acid, the pH had to be lowered to increase the concentrations of hydrogen ions. The dissolution ratio of P in the nitric acid solution at pH 4 could approach that in the citric acid solution at pH 6 for all the tested slags.

$$\begin{aligned} &Fe_3(PO_4)_2 \cdot 8H_2O + 4H^+ = 3Fe^{2+} + 2H_2PO_4^- + 8H_2O \\ &\log K = 3.12 \end{aligned} \quad (4)$$

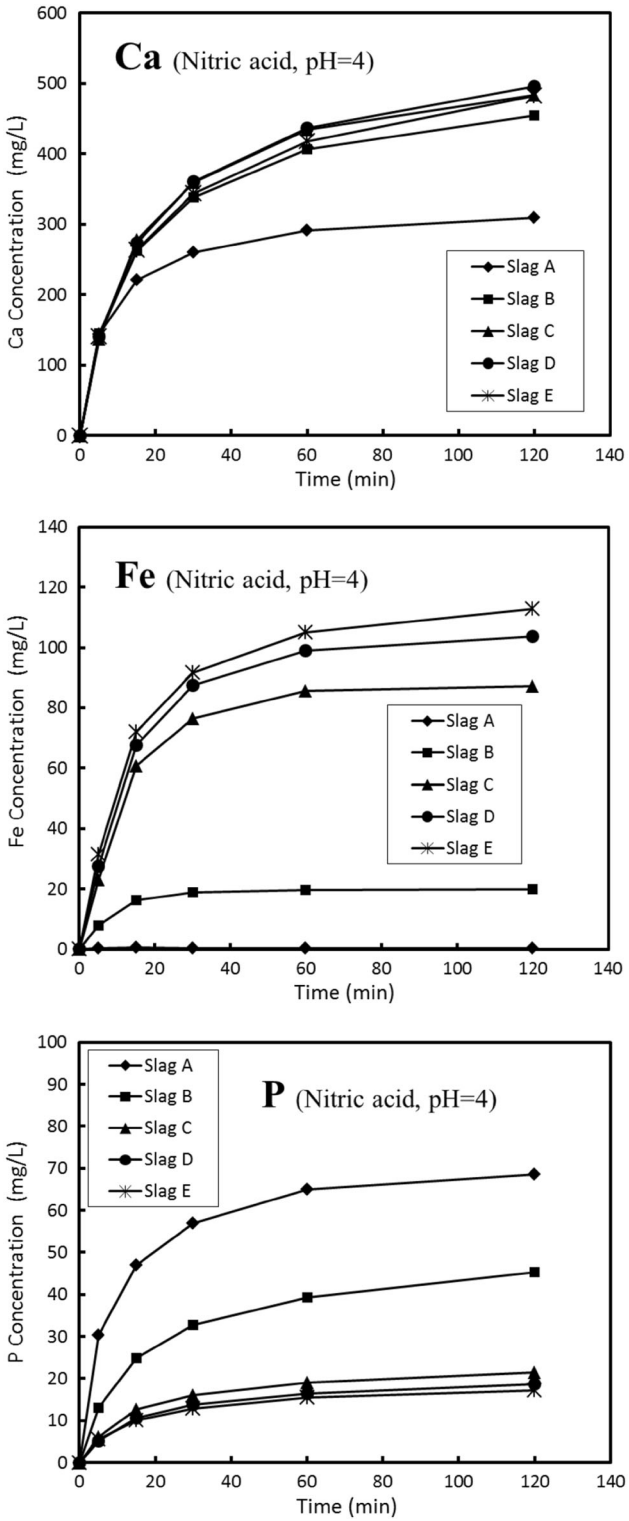

Fig. 6 Changes in Ca, Fe, and P concentrations in the nitric acid solution at pH 4

The dissolution of matrix phase from slag A, which contained only Fe_2O_3, was poor because of the lower Fe concentration. However, for the slags with higher Fe^{2+}/

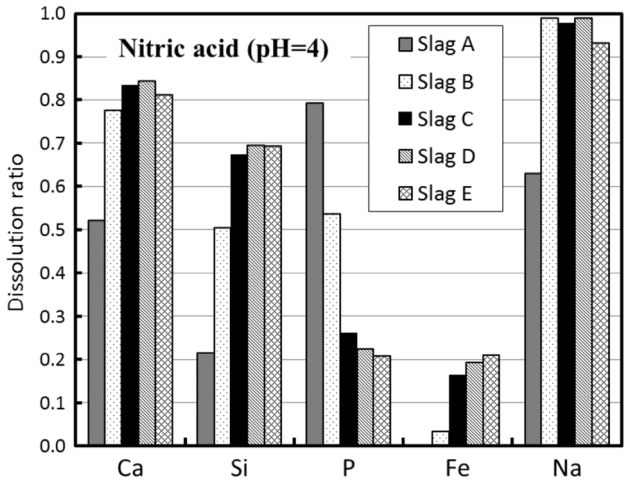

Fig. 7 Dissolution ratios of each element from different slags at pH 4 (nitric acid solution)

T.Fe ratios, the concentration of Fe was comparable to that of Si. Therefore, the possibility of precipitating iron phosphate was discussed. When Fe^{2+} and $H_2PO_4^-$ ions coexist in aqueous solutions, vivianite ($Fe_3(PO_4)_2{\cdot}8H_2O$) could precipitate [26]. The dissolution reaction of vivianite and its equilibrium constant are described by Eq. (4) [26, 27]. Figure 8 shows the calculated relationship between the concentrations of Fe^{2+} and P in aqueous solution at pH 4 and their comparison with the leaching results in the nitric acid solution. For the slags with higher Fe^{2+}/T.Fe ratios, the concentrations of the phosphate and Fe^{2+} ions were close to the solubility line of vivianite, demonstrating that the concentration of P was restricted by the solubility of vivianite. Considering the high dissolution ratios of Ca and Si in this case (as shown in Fig. 7), we concluded that although large amounts of the solid solution and matrix phase were dissolved, the precipitation of the dissolved P occurred resulting in a lower dissolution ratio of P.

The phase fractions in slags with different Fe^{2+}/T.Fe ratios were calculated based on the mass balance and compared with the fractions of the residue and dissolved mass in the nitric acid solution, as shown in Fig. 9. Because of the loss of the aqueous solution during sampling, the total amount of the dissolved mass and residue was less than the initial slag mass. With the increasing Fe^{2+}/T.Fe ratio, the mass fraction of the solid solution increased significantly, and those of the matrix and Fe-rich phases decreased correspondingly. For slag A, the fraction of the dissolved mass was almost the same as that of the solid solution. Because the dissolution of Fe (Fe-containing phases) was insignificant, it was considered that the solid solution was selectively dissolved. When the Fe_2O_3 in slag transformed into FeO, the fraction of the dissolved mass was significantly higher than that of the solid solution. This meant that a large amount of the matrix phase was dissolved, which was not beneficial for the selective leaching of the P-concentrated solid solution.

Figure 10 shows the solubility line of vivianite at pH 6 and the leaching results in the citric acid solution. Although a great deal of Fe^{2+} ions existed, the concentration of P was still high and significantly higher than its saturation concentration. This was because Fe^{2+} ions can form complexes with the citrate ions ($C_6H_5O_7^{3-}$) in the citric acid solution. The formation reaction of the $FeC_6H_5O_7^-$ complex is described by Eq. (5) [26]. The remaining Fe^{2+}, which did not react with the citrate ions, was identified as free Fe^{2+} in the aqueous solution. Because Ca^{2+} can also form complexes, as shown in Eq. (6) [28], the existence of $CaC_6H_5O_7^-$ was also taken into consideration. The concentration of $C_6H_5O_7^{3-}$ was determined using the final volumes of the aqueous solution and the mass of the added citric acid. Using these equations, the concentration of the free Fe^{2+} ions in the citric acid solution was calculated.

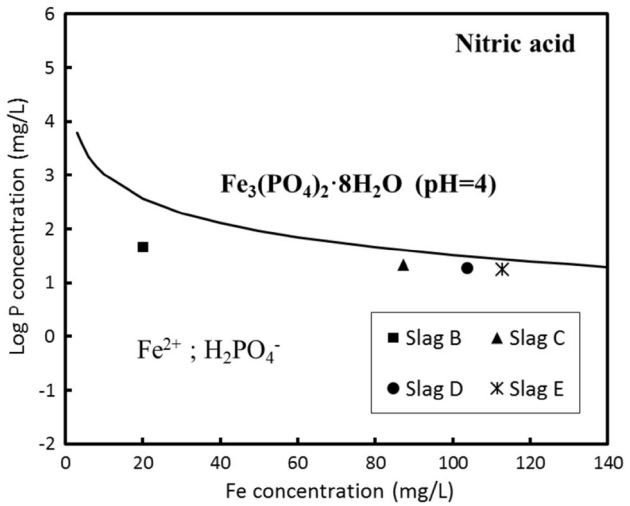

Fig. 8 Solubility line of phosphate precipitate at pH 4 and leaching results in the nitric acid solution

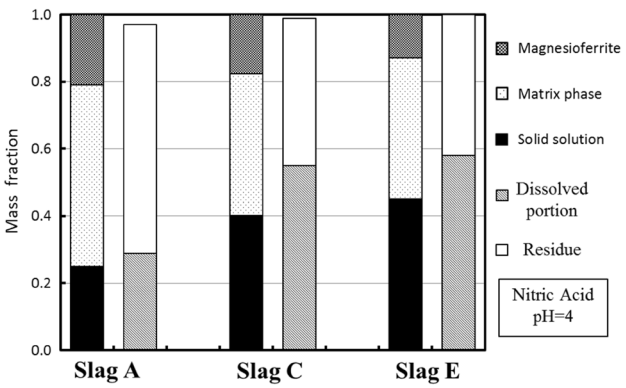

Fig. 9 Fractions of the dissolved mass and residue at pH 4, compared to the phase fractions in the slag

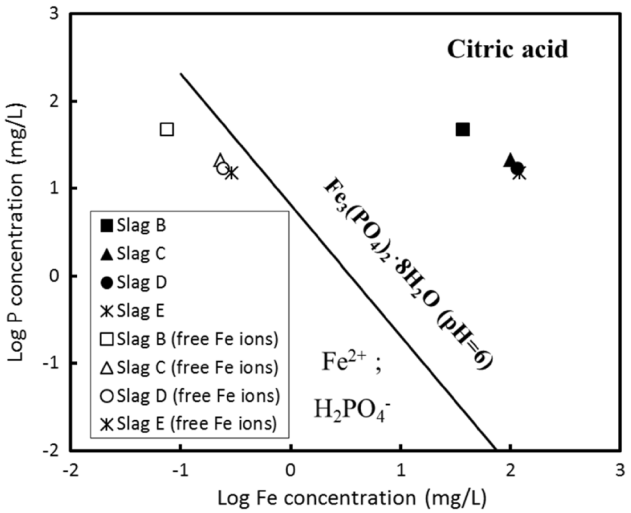

Fig. 10 Solubility line of phosphate precipitate at pH 6 and leaching results in the citric acid solution

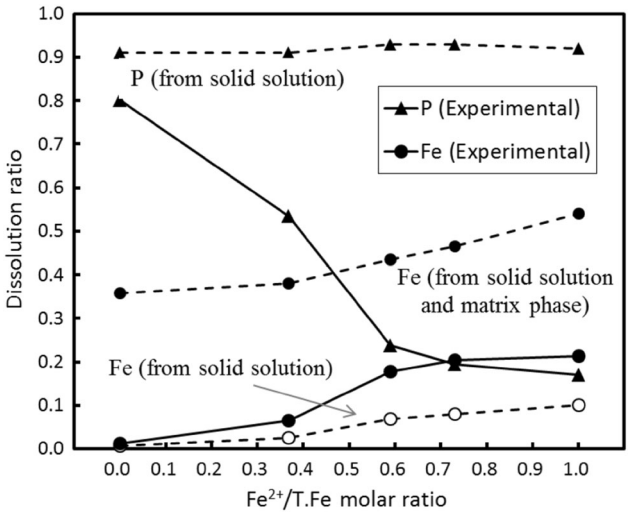

Fig. 11 Calculated dissolution ratios of P and Fe and leaching results in the citric acid solution at pH 6

Figure 10 shows that the concentration of free Fe^{2+} was very low, lower than 0.3 mg/L. The concentrations of P and free Fe^{2+} were located close to the solubility line of vivianite. Because the concentration of the free Fe^{2+} was too low, the amount of phosphate precipitate was negligible. Therefore, most of the dissolved P could exist in stable form in the citric acid solution.

$$Fe^{2+} + C_6H_5O_7^{3-} = FeC_6H_5O_7^{-} \quad \log K = 5.86 \tag{5}$$

$$Ca^{2+} + C_6H_5O_7^{3-} = CaC_6H_5O_7^{-} \quad \log K = 3.22 \tag{6}$$

Assuming that the solid solution or matrix phase was separately dissolved, the dissolution ratios of P and Fe from the slags with different Fe^{2+}/T.Fe ratios were calculated using the mass fractions and compositions of each phase. The calculated dissolution ratio of P was equal to the mass fraction of P distributed in the solid solution. Figure 11 shows the calculated values and experimental results when citric acid was used. The calculated dissolution ratio of P from each slag was approximately 90%, indicating that most of the P was concentrated in the solid solution. For slag A, which contained only Fe_2O_3, the dissolution ratio of P was close to the calculated value. The dissolution ratio of Fe was very low, the same as that calculated from the solid solution. These findings demonstrated that the majority of the solid solution was dissolved without significant dissolution of other phases. A better selective leaching of solid solution was exhibited.

With the increasing Fe^{2+}/T.Fe ratio in slag, the dissolution ratio of P decreased significantly, and became less than 70% when the Fe^{2+}/T.Fe ratio exceeded 0.1. For slags C, D, and E, the dissolution ratios of P were significantly lower than the calculated values. Without considering phosphate precipitation, these results indicated that the dissolution of solid solution was poor. However, the dissolution ratio of Fe was higher than the value calculated from the solid solution and lower than that obtained when the solid solution and matrix phase were both dissolved. This illustrated that some of the dissolved Fe was supplied by the matrix phase. Therefore, when FeO existed in slag, the dissolution of solid solution became difficult, and the dissolution of matrix phase obviously occurred.

The different dissolution behaviors of the mineral phases were attributed to the differences in their mineral structures and bond strengths. In silicate or phosphate minerals, Si and P form tetrahedral units with four O atoms, SiO_4^{4-} and PO_4^{3-}, where metal cations share the O atoms in the corners of the tetrahedral structures [29]. Metal cations and Si or P are combined by metal–O–Si or metal–O–P bonds, respectively. The electrical charges and sizes of the cations determine the strength of the cation–O bonds. Shorter bond lengths and higher electric charges of the metal ions result in higher bond strengths [30]. To consider both the electric charge and the ionic radius simultaneously, the ionization potential (Z/r^2) is often used, as presented in Table 4 [30, 31]. The dissolution of silicate or phosphate minerals in acid solutions depends on the breaking of the weaker bonds in their structure [29]. Because the strength of the P–O or Si–O bonds is significantly higher than that of the metal–O bonds, dissolution would favor the breaking of the metal–O bonds. Thus, the metal dissolves to form metal cations, while P and Si dissolve to form phosphate (PO_4^{3-}) and silicate (SiO_4^{4-}), respectively.

Table 4 Effective ionic radii for cations and anions and their coordination numbers and ionization potentials

Ion	Coordination number	Ionic radius (nm)	Z/r^2 (nm^{-2})
Ca^{2+}	6	0.100	200.0
Fe^{2+}	6	0.061	537.5
Fe^{3+}	6	0.055	991.7
Si^{4+}	4	0.026	5917. 1
P^{5+}	4	0.017	17,301.0
O^{2-}	–	0.140	102.0

As demonstrated by the Hume–Rothery rule [32], if the radii of two different ions are almost similar and the ions have the same valence, then these ions replace each other in solid solutions. As listed in Table 4, Fe^{2+} has the same ionic valence as Ca^{2+}, and its radius is smaller than that of Ca^{2+}. Therefore, Fe^{2+} ions can replace Ca^{2+} and can easily enter the C_2S–C_3P solid solution. This explains the presence of FeO in the solid solution of the slags containing FeO. For the solid solution containing FeO, some Fe–O–P bonds might exist, along with the Ca–O–P bonds. Because the ionization potential of Fe^{2+} is larger than that of Ca^{2+}, the strength of the Fe–O bonds is higher than that of the Ca–O bonds [30]. The Fe–O–P bonds are more difficult to break than the Ca–O–P bonds during leaching. Therefore, the dissolution of the solid solution containing FeO was difficult for slag E.

The matrix phase in these slags was the silicate glass of the CaO–Fe_tO–SiO_2 system. As shown in Fig. 12, Si forms tetrahedral units (SiO_4^{4-}) with four O atoms, and complex networks exist in silicate glass [29]. It has been commonly reported that Fe^{2+} ions act as network modifiers in silicate glass, resulting in octahedral coordination [33]. However, for the CaO–Fe_2O_3–SiO_2 glass, the Fe^{3+} ions are tetrahedrally and octahedrally coordinated [34, 35]. The

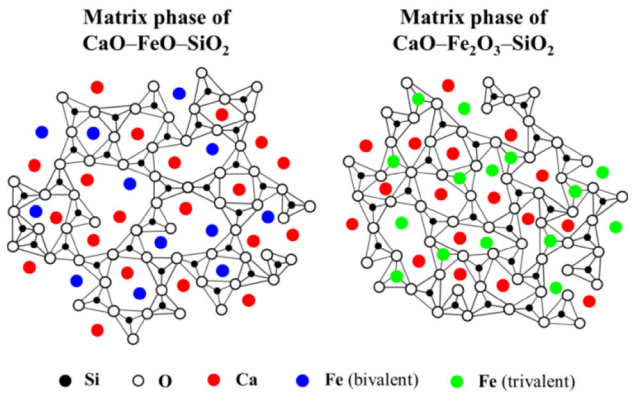

Fig. 12 Schematic illustration of the structure of the CaO–FeO–SiO_2 and CaO–Fe_2O_3–SiO_2 phases (Color figure online)

tetrahedral Fe^{3+} ions act as network formers, similarly to SiO_4^{4-}, while the octahedral Fe^{3+} ions act as network modifiers, similarly to Ca^{2+}. These structures are illustrated in Fig. 12. As listed in Table 4, the ionization potential of Fe^{3+} is larger than that of Fe^{2+}, and thus the bond strength of Fe(ferric)–O is higher. In addition, because the Fe–O bonds formed by tetrahedrally coordinated Fe^{3+} are shorter than those formed by octahedrally coordinated Fe^{3+}, strong tetrahedral Fe(ferric)–O bonds exist. We concluded that the Fe(ferric)–O–Si bonds are more stable than the Fe(ferrous)–O–Si bonds in silicate glass. Therefore, the dissolution of the CaO–Fe_2O_3–SiO_2 phase in aqueous solutions was difficult compared to that of the CaO–FeO–SiO_2 phase.

Residue Composition

The mineralogical compositions of the residues obtained after leaching were analyzed using XRD, as shown in Fig. 13. The peaks associated with the solid solution and Fe-rich phase (hematite or wüstite) were observed in the original slags. For slag A, the peaks associated with the solid solution almost disappeared after leaching in the citric or nitric acid solution, while the peaks of hematite intensified. This demonstrated that the solid solution was separated from slag by selective leaching, while the Fe-rich phase remained. The peaks associated with the solid solution still existed in the residue of slag E, indicating that the dissolution of solid solution was poor. When slag E was leached by nitric acid at pH 4, the intensities of the peaks of the solid solution in the residue were lower and those of wüstite higher compared to those in the citric acid solution at pH 6. This illustrated that more solid solution was dissolved, but the dissolution of solid solution was still insufficient.

Table 5 lists the average compositions of the residues after leaching in the citric acid solution at pH 6. When only Fe_2O_3 existed in slag, due to a better selective leaching of P, the P_2O_5 content in the residue was only 1.7 mass%, and half of the residue consisted of Fe_2O_3. This residue has the potential to be reused for steelmaking. With the increasing Fe^{2+}/T.Fe ratio in slag, the P_2O_5 content in the residue increased while the Fe_tO content decreased. The P_2O_5 contents in the residues of slags with higher Fe^{2+}/T.Fe ratios were higher than the P_2O_5 contents in the original slags. This indicated that the dissolution of P was difficult compared with those of other elements. These results were consistent with the above XRD results.

Figure 14 shows the EPMA images of the surface of the residue after leaching in the citric acid solution. The compositions of the identified domains on the surface of the residue are listed in Table 6. Two phases, similar in composition to the matrix phase and hematite, were

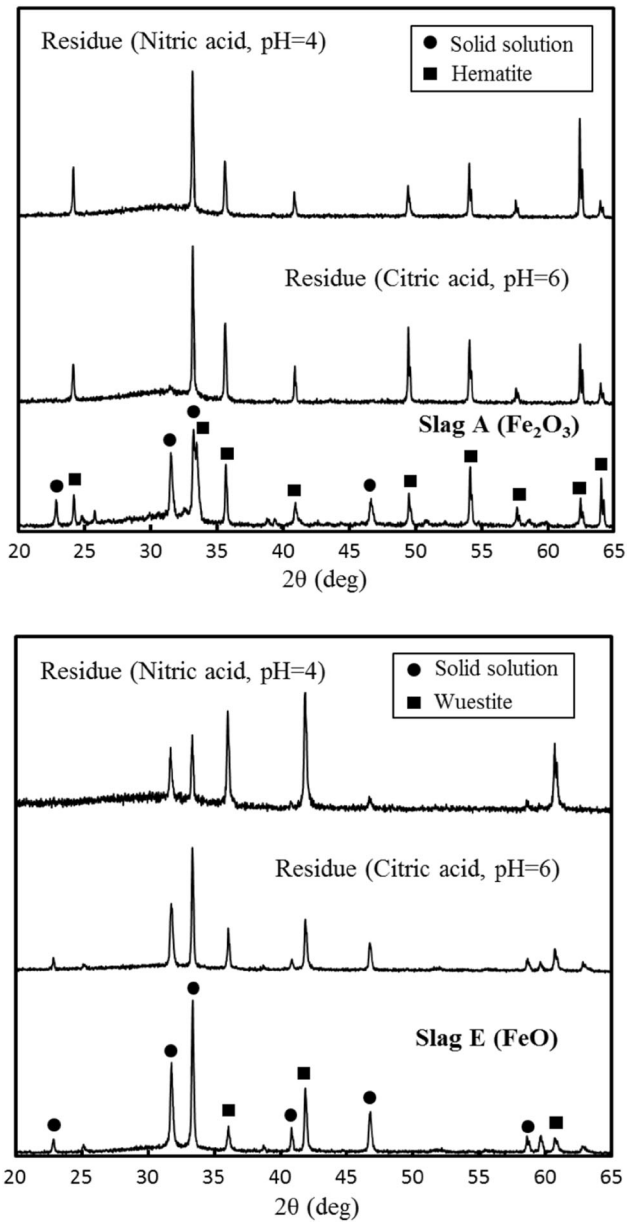

Fig. 13 XRD patterns of slags with different Fe valences and their residues

Table 5 Compositions of residues after leaching in the citric acid solution at pH 6 (mass %)

Residue	CaO	SiO_2	Fe_tO	P_2O_5	Na_2O
Slag A	24.7	22.4	48.5	1.7	2.7
Slag B	27.9	22.7	41.0	5.8	2.6
Slag C	29.3	18.6	40.2	8.7	3.2
Slag D	29.7	20.1	37.9	9.1	3.2
Slag E	30.8	20.0	36.2	9.9	3.0

observed on the surface of the residue of slag A. It was difficult to detect the solid solution for this residue, which indicated that the solid solution that came in contact with the aqueous solution dissolved selectively. Aside from wüstite and matrix phase, a domain with high P_2O_5 content was also observed for slag E. Its composition was similar with that of the solid solution, demonstrating that the solid solution did not sufficiently dissolve.

In summary, the existence of FeO in slag deteriorated the dissolution of the P-concentrated solid solution and caused the dissolution of the Fe-containing matrix phase. To achieve a better selective leaching of P from slag, the practical steelmaking slag should be oxidized to decrease the Fe^{2+}/T.Fe ratio in slag below 0.1. Moreover, the oxidization of steelmaking slag has been successfully industrialized to modify slag with the aid of blowing oxygen [36].

Conclusions

To determine the appropriate slag composition for selective leaching, it was necessary to clarify the influence of the Fe^{2+}/T.Fe ratio in slag on the dissolution behavior of P and Fe. In this study, we synthesized five types of slags with different Fe^{2+}/T.Fe ratios and investigated their dissolution behaviors. The following conclusions were drawn:

(1) With the increasing Fe^{2+}/T.Fe ratio in slag, the P_2O_5 content in the solid solution decreased, while the Fe_tO content increased. Although the distribution ratio of P_2O_5 between the solid solution and matrix phase decreased, the mass fraction of the solid solution in slag increased. Most of the P was still concentrated in the solid solution.

(2) Citric acid showed an enhanced capacity to dissolve P from slag. Approximately 80% of P was dissolved from the slag containing only Fe_2O_3 at pH 6. When nitric acid is used as leaching agent, to achieve a similar leaching performance, leaching should be conducted at a lower pH.

(3) Because the presence of FeO in the solid solution deteriorated its dissolution, the dissolution ratio of P decreased significantly with the increasing Fe^{2+}/T.Fe ratio in slag. By contrast, the dissolution of Fe was promoted. This was attributed to a larger dissolution of the CaO–FeO–SiO_2 matrix phase compared with the CaO–Fe_2O_3–SiO_2 matrix phase. Therefore, to achieve a better selective leaching of P, steelmaking slag should be oxidized in order to lower the Fe^{2+}/T.Fe ratio in slag below 0.1.

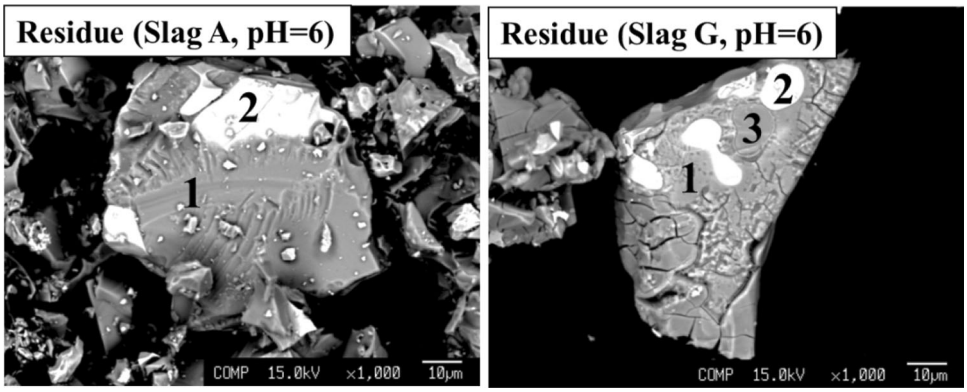

Fig. 14 EPMA images of the surface of the residue after leaching in the citric acid solution at pH 6 (1: matrix phase, 2: Fe-rich phase, 3: P-rich phase)

Table 6 Average compositions of some phases on the surface of the residue after leaching (mass%)

		CaO	SiO_2	Fe_tO	P_2O_5	Na_2O
Residue (Slag A)	1	36.7	38.6	19.9	1.7	3.2
	2	0.5	0.3	99.1	0.0	0.0
Residue (Slag E)	1	19.4	42.6	33.3	4.1	0.5
	2	0.7	0.4	98.7	0.1	0.1
	3	41.6	26.7	12.8	16.2	2.7

Compliance with Ethical Standards

Conflict of interest On behalf of all authors, the corresponding author states that there is no conflict of interest.

References

1. Cheng CY, Misra VN, Clough J, Muni R (1999) Dephosphorisation of western Australian iron ore by hydrometallurgical process. Miner Eng 12:1083–1092
2. Fisher-white MJ, Lovel RR, Sparrow GJ (2012) Heat and acid leach treatments to lower phosphorus levels in goethitic iron ores. ISIJ Int 52:1794–1800
3. Yu J, Guo Z, Tang H (2013) Dephosphorization treatment of high phosphorus oolitic iron ore by hydrometallurgical process and leaching kinetics. ISIJ Int 53:2056–2064
4. Matinde E, Hino M (2011) Dephosphorization treatment of high phosphorus iron ore by pre-reduction, air jet milling and screening methods. ISIJ Int 51:544–551
5. Fix W, Heymann H, Heinke R (1969) Subsolidus relations in the system $2CaO{\cdot}SiO_2$–$3CaO{\cdot}P_2O_5$. J Am Ceram Soc 52:346–347
6. Ito K, Yanagisawa M, Sano N (1982) Phosphorus distribution between solid $2CaO{\cdot}SiO_2$ and molten CaO–SiO_2–FeO–Fe_2O_3 slags. Tetsu-to-Hagane 68:342–344
7. Tripathy PK, Banerjee A, Singh B, Das D, Das AK (2008) Approaches for conversion of high phosphorus hot metal to steel for flat products. ISIJ Int 48:578–583
8. Mukherjee T, Chatterjee A (1996) Production of low phosphorus steels from high phosphorus Indian hot metal: experience at Tata Steel. Bull Mater Sci 19:893–903
9. Kitamura S, Pahlevani F (2014) Process simulation of dephosphorization treatment of hot metal with high phosphorus content. Tetsu-to-Hagane 100:500–508
10. Pak JJ, Fruehan RJ (1991) The effect of Na_2O on dephosphorization by CaO-Based steelmaking slags. Metall Trans B 22:39–46
11. Du C, Gao X, Ueda S, Kitamura S (2018) Distribution of P_2O_5 and Na_2O between solid solution and liquid phase in the CaO–SiO_2–Fe_2O_3–P_2O_5–Na_2O slag system with high P_2O_5 content. Metall Mater Trans B 49:181–189
12. Li HJ, Suito H, Tokuda M (1995) Thermodynamic analysis of slag recycling using a slag regenerator. ISIJ Int 35:1079–1088
13. Yokoyama K, Kubo H, Mori K, Okada H, Takeuchi S, Nagasaka T (2007) Separation and recovery of phosphorus from steelmaking slags with the aid of a strong magnetic field. ISIJ Int 47:1541–1548
14. Teratoko T, Maruoka N, Shibata H, Kitamura S (2012) Dissolution behavior of dicalcium silicate and tricalcium phosphate solid solution and other phases of steelmaking slag in an aqueous solution. High Temp Mater Proc 31:329–338
15. Numata M, Maruoka N, Kim SJ, Kitamura S (2014) Fundamental experiment to extract phosphorous selectively from steelmaking slag by leaching. ISIJ Int 54:1983–1990
16. Nielsson FT (1987) Manual of fertilizer processing. Marcel Dekker, New York
17. Du C, Gao X, Ueda S, Kitamura S (2017) Effects of cooling rate and acid on extracting soluble phosphorus from slag with high P_2O_5 content by selective leaching. ISIJ Int 57:487–496
18. Du C, Gao X, Ueda S, Kitamura S (2017) Effect of Na_2O addition on phosphorus dissolution from steelmaking slag with high P_2O_5 content. J Sustain Metall 3:671–682
19. Du C, Gao X, Ueda S, Kitamura S (2018) Recovery of phosphorus from modified steelmaking slag with high P_2O_5 content via leaching and precipitation. ISIJ Int 58:833–841
20. Du C, Gao X, Ueda S, Kitamura S (2018) Optimum conditions for phosphorus recovery from steelmaking slag with high P_2O_5 content by selective leaching. ISIJ Int 58:860–868
21. Gao X, Maruok N, Kim SJ, Ueda S, Kitamura S (2015) Dissolution behavior of nutrient elements from fertilizer made of steelmaking slag in an irrigated paddy field environment. J Sustain Metall 1:304–313
22. Ban-ya S (2000) Ferrous process metallurgy. The Japan Institute of Metals, Maruzen Publishing, Tokyo
23. Turkdogan ET (1980) Physical chemistry of high temperature technology. Academic Press, New York
24. Saikkonen RJ, Rautiainen IA (1993) Determination of ferrous iron in rock and mineral samples by three volumetric methods. Bull Geol Soc Finl Part I 65:59–64

25. McDonald RG, Whittington BI (2008) Atmospheric acid leaching of nickel laterites review. Part II. Chloride and bio-technologies. Hydrometallurgy 91:56–69
26. Markich SJ, Brown PL (1999) Thermochemical data for environmentally-relevant elements. ANSTO Environment Division, NSW
27. Futatsuka T, Shitogiden K, Miki T, Nagasaka T, Hino M (2004) Dissolution behavior of nutrition elements from steelmaking slag into seawater. ISIJ Int 44:753–761
28. Muus J, Lebel H (1936) On complex calcium citrate. Mathematisk-fysiske Meddelelser XIII 19:1–17
29. Crundwell FK (2014) The mechanism of dissolution of minerals in acidic and alkaline solutions: part II application of a new theory to silicates, aluminosilicates and quartz. Hydrometallurgy 149:265–275
30. Sohn I, Min DJ (2012) A review of the relationship between viscosity and the structure of calcium-silicate-based slags in ironmaking. Steel Res 83:611–630
31. Shannon RD (1976) Revised effective ionic radii and systematic studies of interatomic distances in halides and chalcogenides. Acta Cryst A32:751–767
32. Mizutani U (2010) Hume-Rothery rules for structurally complex alloy phases. Taylor & Francis, USA
33. Pargamin L, Lupis CHP, Flinn PA (1972) Mössbauer analysis of the distribution of iron cations in silicate slags. Metall Trans 3:2093–2105
34. Iwamoto N, Tsunawaki Y, Nakagawa H, Yoshimura T, Wakabayashi N (1978) Investigation of calcium-iron-silicate glasses by the Mössbauer method. J Non-Cryst Solids 29:347–356
35. Nagata K, Hayashi M (2001) Structure relaxation of silicate melts containing iron oxide. J Non-Cryst Solids 282:1–6
36. Tseng YH, Lee YC, Sheu BL (2015) Application and breakthrough of BOF slag modification technique. China Steel Tech Rep 28:46–51